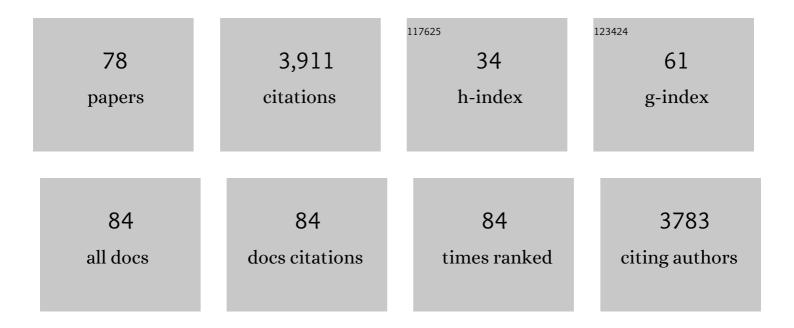
Roshanak Darvishzadeh

List of Publications by Year in descending order

Source: https://exaly.com/author-pdf/1202758/publications.pdf Version: 2024-02-01



#	Article	IF	CITATIONS
1	Cropping Patterns of Annual Crops: A Remote Sensing Review. Remote Sensing, 2022, 14, 2404.	4.0	18
2	Mapping leaf area index in a mixed temperate forest using Fenix airborne hyperspectral data and Gaussian processes regression. International Journal of Applied Earth Observation and Geoinformation, 2021, 95, 102242.	2.8	16
3	Machine learning methods' performance in radiative transfer model inversion to retrieve plant traits from Sentinel-2 data of a mixed mountain forest. International Journal of Digital Earth, 2021, 14, 106-120.	3.9	27
4	Canopy chlorophyll content retrieved from time series remote sensing data as a proxy for detecting bark beetle infestation. Remote Sensing Applications: Society and Environment, 2021, 22, 100524.	1.5	3
5	Priority list of biodiversity metrics to observe from space. Nature Ecology and Evolution, 2021, 5, 896-906.	7.8	101
6	Mapping of wheat lodging susceptibility with synthetic aperture radar data. Remote Sensing of Environment, 2021, 259, 112427.	11.0	15
7	A laboratory for conceiving Essential Biodiversity Variables (EBVs)—The â€~Data pool initiative for the Bohemian Forest Ecosystem'. Methods in Ecology and Evolution, 2021, 12, 2073-2083.	5.2	4
8	Forest Leaf Mass per Area (LMA) through the Eye of Optical Remote Sensing: A Review and Future Outlook. Remote Sensing, 2021, 13, 3352.	4.0	13
9	Mapping saffron fields and their ages with Sentinel-2 time series in north-east Iran. International Journal of Applied Earth Observation and Geoinformation, 2021, 102, 102398.	2.8	3
10	Thermal infrared remote sensing of vegetation: Current status and perspectives. International Journal of Applied Earth Observation and Geoinformation, 2021, 102, 102415.	2.8	15
11	Estimation of crop angle of inclination for lodged wheat using multi-sensor SAR data. Remote Sensing of Environment, 2020, 236, 111488.	11.0	45
12	Effects of prediction accuracy of the proportion of vegetation cover on land surface emissivity and temperature using the NDVI threshold method. International Journal of Applied Earth Observation and Geoinformation, 2020, 85, 101984.	2.8	47
13	Comparing methods for mapping canopy chlorophyll content in a mixed mountain forest using Sentinel-2 data. International Journal of Applied Earth Observation and Geoinformation, 2020, 87, 102037.	2.8	42
14	Special Issue "Hyperspectral Remote Sensing of Agriculture and Vegetation― Remote Sensing, 2020, 12, 3665.	4.0	20
15	Mapping Canopy Chlorophyll Content in a Temperate Forest Using Airborne Hyperspectral Data. Remote Sensing, 2020, 12, 3573.	4.0	19
16	Evaluating Prediction Models for Mapping Canopy Chlorophyll Content Across Biomes. Remote Sensing, 2020, 12, 1788.	4.0	7
17	Understanding wheat lodging using multi-temporal Sentinel-1 and Sentinel-2 data. Remote Sensing of Environment, 2020, 243, 111804.	11.0	45
18	Discriminant analysis for lodging severity classification in wheat using RADARSAT-2 and Sentinel-1 data. ISPRS Journal of Photogrammetry and Remote Sensing, 2020, 164, 138-151.	11.1	25

#	Article	IF	CITATIONS
19	Sentinelâ€2 accurately maps greenâ€attack stage of European spruce bark beetle (<i>Ips typographus</i> , L.) compared with Landsatâ€8. Remote Sensing in Ecology and Conservation, 2019, 5, 87-106.	4.3	95
20	Timing of red-edge and shortwave infrared reflectance critical for early stress detection induced by bark beetle (Ips typographus, L.) attack. International Journal of Applied Earth Observation and Geoinformation, 2019, 82, 101900.	2.8	22
21	Evaluating the performance of PROSPECT in the retrieval of leaf traits across canopy throughout the growing season. International Journal of Applied Earth Observation and Geoinformation, 2019, 83, 101919.	2.8	12
22	Accurate modelling of canopy traits from seasonal Sentinel-2 imagery based on the vertical distribution of leaf traits. ISPRS Journal of Photogrammetry and Remote Sensing, 2019, 157, 108-123.	11.1	31
23	Validating the Predictive Power of Statistical Models in Retrieving Leaf Dry Matter Content of a Coastal Wetland from a Sentinel-2 Image. Remote Sensing, 2019, 11, 1936.	4.0	6
24	Analysis of Sentinel-2 and RapidEye for Retrieval of Leaf Area Index in a Saltmarsh Using a Radiative Transfer Model. Remote Sensing, 2019, 11, 671.	4.0	44
25	Integration of Landsat-8 Thermal and Visible-Short Wave Infrared Data for Improving Prediction Accuracy of Forest Leaf Area Index. Remote Sensing, 2019, 11, 390.	4.0	15
26	Remote sensing-based crop lodging assessment: Current status and perspectives. ISPRS Journal of Photogrammetry and Remote Sensing, 2019, 151, 124-140.	11.1	83
27	Mapping leaf chlorophyll content from Sentinel-2 and RapidEye data in spruce stands using the invertible forest reflectance model. International Journal of Applied Earth Observation and Geoinformation, 2019, 79, 58-70.	2.8	57
28	Sensitivity of Landsat-8 OLI and TIRS Data to Foliar Properties of Early Stage Bark Beetle (Ips) Tj ETQq0 0 0 rgBT /	Overlock 1 4.0	.0 ₃₃ 50 382
29	Estimation of forest leaf water content through inversion of a radiative transfer model from LiDAR and hyperspectral data. International Journal of Applied Earth Observation and Geoinformation, 2019, 74, 120-129.	2.8	17
30	Leaf to canopy upscaling approach affects the estimation of canopy traits. GIScience and Remote Sensing, 2019, 56, 554-575.	5.9	27
31	Discriminating transplanted and direct seeded rice using Sentinel-1 intensity data. International Journal of Applied Earth Observation and Geoinformation, 2019, 76, 143-153.	2.8	26
32	Mapping forest canopy nitrogen content by inversion of coupled leaf-canopy radiative transfer models from airborne hyperspectral imagery. Agricultural and Forest Meteorology, 2018, 253-254, 247-260.	4.8	67
33	Vegetation phenology from Sentinel-2 and field cameras for a Dutch barrier island. Remote Sensing of Environment, 2018, 215, 517-529.	11.0	153
34	European spruce bark beetle (Ips typographus, L.) green attack affects foliar reflectance and biochemical properties. International Journal of Applied Earth Observation and Geoinformation, 2018, 64, 199-209.	2.8	71
35	Foliar and woody materials discriminated using terrestrial LiDAR in a mixed natural forest. International Journal of Applied Earth Observation and Geoinformation, 2018, 64, 43-50.	2.8	61
36	Assessing trends and seasonal changes in elephant poaching risk at the small area level using spatio-temporal Bayesian modeling. International Journal of Geographical Information Science, 2018, 32, 622-636.	4.8	5

#	Article	IF	CITATIONS
37	Improving leaf area index (LAI) estimation by correcting for clumping and woody effects using terrestrial laser scanning. Agricultural and Forest Meteorology, 2018, 263, 276-286.	4.8	70
38	Machine Learning Using Hyperspectral Data Inaccurately Predicts Plant Traits Under Spatial Dependency. Remote Sensing, 2018, 10, 1263.	4.0	22
39	Impact of Vertical Canopy Position on Leaf Spectral Properties and Traits across Multiple Species. Remote Sensing, 2018, 10, 346.	4.0	35
40	Specific leaf area estimation from leaf and canopy reflectance through optimization and validation of vegetation indices. Agricultural and Forest Meteorology, 2017, 236, 162-174.	4.8	40
41	Spatially detailed retrievals of spring phenology from single-season high-resolution image time series. International Journal of Applied Earth Observation and Geoinformation, 2017, 59, 19-30.	2.8	32
42	Retrieval of Specific Leaf Area From Landsat-8 Surface Reflectance Data Using Statistical and Physical Models. IEEE Journal of Selected Topics in Applied Earth Observations and Remote Sensing, 2017, 10, 3529-3536.	4.9	28
43	The NaÃ ⁻ ve Overfitting Index Selection (NOIS): A new method to optimize model complexity for hyperspectral data. ISPRS Journal of Photogrammetry and Remote Sensing, 2017, 133, 61-74.	11.1	16
44	Retrieving vegetation canopy water content from hyperspectral thermal measurements. Agricultural and Forest Meteorology, 2017, 247, 365-375.	4.8	26
45	Expert system for modelling stopover site selection by barnacle geese. Ecological Modelling, 2017, 359, 398-405.	2.5	3
46	Canopy leaf water content estimated using terrestrial LiDAR. Agricultural and Forest Meteorology, 2017, 232, 152-162.	4.8	46
47	Canopy foliar nitrogen retrieved from airborne hyperspectral imagery by correcting for canopy structure effects. International Journal of Applied Earth Observation and Geoinformation, 2017, 54, 84-94.	2.8	35
48	Vegetation Indices for Mapping Canopy Foliar Nitrogen in a Mixed Temperate Forest. Remote Sensing, 2016, 8, 491.	4.0	63
49	Environmental parameters linked to the last migratory stage of barnacle geese en route to their breeding sites. Animal Behaviour, 2016, 118, 81-95.	1.9	12
50	Retrieval of vertical leaf water content using terrestrial full-waveform lidar. Proceedings of SPIE, 2016, , .	0.8	0
51	Simple and robust methods for remote sensing of canopy chlorophyll content: a comparative analysis of hyperspectral data for different types of vegetation. Plant, Cell and Environment, 2016, 39, 2609-2623.	5.7	109
52	Retrieval of leaf area index in different plant species using thermal hyperspectral data. ISPRS Journal of Photogrammetry and Remote Sensing, 2016, 119, 390-401.	11.1	50
53	Elephant poaching risk assessed using spatial and non-spatial Bayesian models. Ecological Modelling, 2016, 338, 60-68.	2.5	13
54	Measuring the response of canopy emissivity spectra to leaf area index variation using thermal hyperspectral data. International Journal of Applied Earth Observation and Geoinformation, 2016, 53, 40-47.	2.8	15

#	Article	IF	CITATIONS
55	Retrieval of forest leaf functional traits from HySpex imagery using radiative transfer models and continuous wavelet analysis. ISPRS Journal of Photogrammetry and Remote Sensing, 2016, 122, 68-80.	11.1	41
56	Estimating leaf functional traits by inversion of PROSPECT: Assessing leaf dry matter content and specific leaf area in mixed mountainous forest. International Journal of Applied Earth Observation and Geoinformation, 2016, 45, 66-76.	2.8	83
57	Effects of Canopy Structural Variables on Retrieval of Leaf Dry Matter Content and Specific Leaf Area From Remotely Sensed Data. IEEE Journal of Selected Topics in Applied Earth Observations and Remote Sensing, 2016, 9, 898-909.	4.9	29
58	3D leaf water content mapping using terrestrial laser scanner backscatter intensity with radiometric correction. ISPRS Journal of Photogrammetry and Remote Sensing, 2015, 110, 14-23.	11.1	60
59	Satellite- versus temperature-derived green wave indices for predicting the timing of spring migration of avian herbivores. Ecological Indicators, 2015, 58, 322-331.	6.3	24
60	Comparative analysis of different retrieval methods for mapping grassland leaf area index using airborne imaging spectroscopy. International Journal of Applied Earth Observation and Geoinformation, 2015, 43, 19-31.	2.8	111
61	Leaf Nitrogen Content Indirectly Estimated by Leaf Traits Derived From the PROSPECT Model. IEEE Journal of Selected Topics in Applied Earth Observations and Remote Sensing, 2015, 8, 3172-3182.	4.9	73
62	Applicability of the PROSPECT model for estimating protein and cellulose + lignin in fresh leaves. Remote Sensing of Environment, 2015, 168, 205-218.	11.0	93
63	Spatial and spatiotemporal clustering methods for detecting elephant poaching hotspots. Ecological Modelling, 2015, 297, 180-186.	2.5	28
64	Comparative analysis of different uni- and multi-variate methods for estimation of vegetation water content using hyper-spectral measurements. International Journal of Applied Earth Observation and Geoinformation, 2014, 26, 1-11.	2.8	92
65	Suitability and adaptation of PROSAIL radiative transfer model for hyperspectral grassland studies. Remote Sensing Letters, 2013, 4, 55-64.	1.4	48
66	Inversion of a Radiative Transfer Model for Estimation of Rice Canopy Chlorophyll Content Using a Lookup-Table Approach. IEEE Journal of Selected Topics in Applied Earth Observations and Remote Sensing, 2012, 5, 1222-1230.	4.9	94
67	Why confining to vegetation indices? Exploiting the potential of improved spectral observations using radiative transfer models. Proceedings of SPIE, 2011, , .	0.8	18
68	Mapping grassland leaf area index with airborne hyperspectral imagery: A comparison study of statistical approaches and inversion of radiative transfer models. ISPRS Journal of Photogrammetry and Remote Sensing, 2011, 66, 894-906.	11.1	170
69	Estimation of vegetation fraction in arid areas using ALOS imagery. , 2010, , .		2
70	Leaf Area Index derivation from hyperspectral vegetation indicesand the red edge position. International Journal of Remote Sensing, 2009, 30, 6199-6218.	2.9	100
71	Inversion of a radiative transfer model for estimating vegetation LAI and chlorophyll in a heterogeneous grassland. Remote Sensing of Environment, 2008, 112, 2592-2604.	11.0	459
72	LAI and chlorophyll estimation for a heterogeneous grassland using hyperspectral measurements. ISPRS Journal of Photogrammetry and Remote Sensing, 2008, 63, 409-426.	11.1	328

#	Article	IF	CITATIONS
73	Estimation of vegetation LAI from hyperspectral reflectance data: Effects of soil type and plant architecture. International Journal of Applied Earth Observation and Geoinformation, 2008, 10, 358-373.	2.8	106
74	LEAF AREA INDEX RETRIEVED FROM THERMAL HYPERSPECTRAL DATA. International Archives of the Photogrammetry, Remote Sensing and Spatial Information Sciences - ISPRS Archives, 0, XLI-B7, 99-105.	0.2	2
75	WHEAT LODGING ASSESSMENT USING MULTISPECTRAL UAV DATA. International Archives of the Photogrammetry, Remote Sensing and Spatial Information Sciences - ISPRS Archives, 0, XLII-2/W13, 235-240.	0.2	25
76	Prospect inversion for indirect estimation of leaf dry matter content and specific leaf area. International Archives of the Photogrammetry, Remote Sensing and Spatial Information Sciences - ISPRS Archives, 0, XL-7/W3, 277-284.	0.2	6
77	LEAF AREA INDEX RETRIEVED FROM THERMAL HYPERSPECTRAL DATA. International Archives of the Photogrammetry, Remote Sensing and Spatial Information Sciences - ISPRS Archives, 0, XLI-B7, 99-105.	0.2	1
78	UNDERSTANDING OF CROP LODGING INDUCED CHANGES IN SCATTERING MECHANISMS USING RADARSAT-2 AND SENTINEL-1 DERIVED METRICS. International Archives of the Photogrammetry, Remote Sensing and Spatial Information Sciences - ISPRS Archives, 0, XLIII-B3-2020, 267-274.	0.2	0